

# Diversity of discrete breathers observed in a Josephson ladder

P. Binder, D. Abraimov, and A. V. Ustinov

*Physikalisches Institut III, Universität Erlangen-Nürnberg, Erwin-Rommel-Straße 1, D-91058 Erlangen, Germany*  
(November 21, 2018)

We generate and observe discrete rotobreathers in Josephson junction ladders with open boundaries. Rotobreathers are localized excitations that persist under the action of a spatially uniform force. We find a rich variety of stable dynamic states including pure symmetric, pure asymmetric, and mixed states. The parameter range where the discrete breathers are observed in our experiment is limited by retrapping due to dissipation.

05.45.-a, 63.20.Ry, 74.50.+r

Nonlinearity and lattice discreteness lead to a generic class of excitations that are spatially localized on the scale comparable to the lattice constant. These excitations, also known as *discrete breathers*, have recently attracted a lot of interest in theory of nonlinear lattices<sup>1,2</sup>. It is believed that discrete breathers might play an important role in the dynamics of various physical systems consisting of coupled nonlinear oscillators. It has been even said that that for discrete nonlinear systems breathers might be as important as solitons are for the continuous nonlinear media.

There have been several recent experiments that reported on generation and detection of discrete breathers in diverse systems. These are low-dimensional crystals<sup>3</sup>, anti-ferromagnetic materials<sup>4</sup>, coupled optical waveguides<sup>5</sup>, and Josephson junction arrays<sup>6,7</sup>. By using the method of low temperature scanning laser microscopy, we have recently reported the first direct visualization of discrete breathers<sup>7</sup>.

In this paper we present new measurements of localized modes in Josephson ladders. Using the same method as in our first experiment, we study an even more tightly coupled lattice of Josephson junctions and observe a rich diversity of localized excitations that persist under the action of a spatially uniform force.

A biased Josephson junction behaves very similar to its mechanical analog that is a forced and damped pendulum. An electric bias current flowing across the junction is analogous to a torque applied to the pendulum. The maximum torque that the pendulum can sustain and remain static corresponds to the critical current  $I_c$  of the junction. For low damping and bias below  $I_c$ , the junction allows for two states: the superconducting (static) state and the resistive (rotating) state. The phase difference  $\varphi$  of the macroscopic wave functions of the superconducting islands on both sides of the junction plays the role of an angle coordinate of the pendulum. According to the Josephson relation, a junction in a rotating state generates dc voltage  $V = \frac{1}{2\pi} \Phi_0 \left\langle \frac{d\varphi}{dt} \right\rangle$ , where  $\langle \dots \rangle$  is the time average. By connecting many Josephson junctions by superconducting leads one gets an array of coupled nonlinear oscillators.

We perform experiments with a particular type of

Josephson junction array called Josephson ladder. Theoretical studies<sup>8-10</sup> of these systems have predicted the existence of spatially localized excitations called rotobreathers. Rotobreathers are  $2\pi$ -periodic solutions in time that are exponentially localized in space.

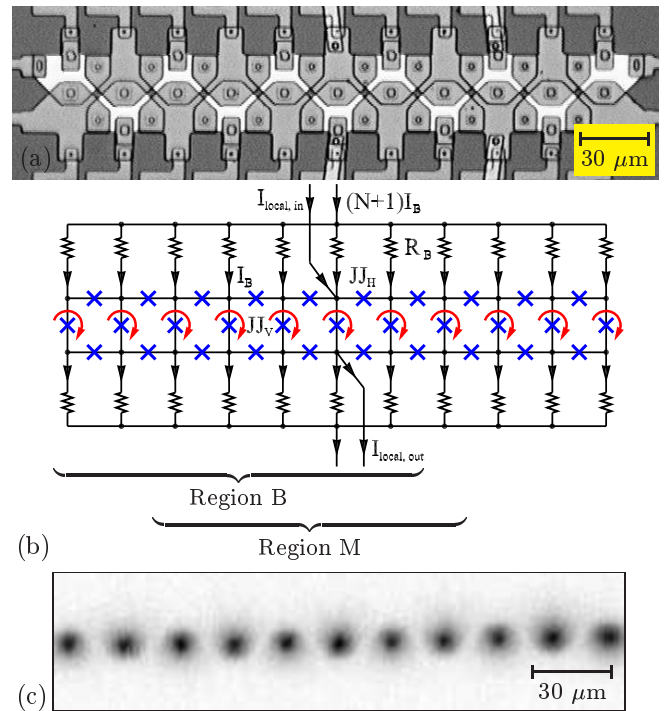


FIG. 1. Optical (a) and schematic (b) view of a linear ladder. (c) Spatially homogeneous whirling state measured by the laser scanning technique.

Measurements are performed on linear ladders (with open boundaries) consisting of Nb/Al-AIO<sub>x</sub>/Nb underdamped Josephson tunnel junctions<sup>11</sup>. An optical image Fig. 1(a) shows a linear ladder that is schematically sketched in Fig. 1(b). Each cell contains 4 small Josephson junctions. The size of the hole between the superconducting electrodes which form the cell is about  $3 \times 3 \mu\text{m}^2$ . The distance between the Josephson junctions is about  $24 \mu\text{m}$ . The number of cells  $N$  in the ladder is 10. Measurements presented in this paper have been performed at 5.2

K. The bias current  $I_B$  was uniformly injected at every node via thin-film resistors  $R_B = 32 \Omega$ . Here we define *vertical junctions* ( $JJ_V$ ) as those in the direction of the external bias current, and *horizontal junctions* ( $JJ_H$ ) as those transverse to the bias. The ladder voltage was read across the central vertical junction. The damping coefficient  $\alpha = \sqrt{\Phi_0/(2\pi I_c C R_{sg}^2)}$  is the same for all junctions as their capacitance  $C$  and sub-gap resistance  $R_{sg}$  scale with the area and  $C_H/C_V = R_{sgV}/R_{sgH}$ . The damping  $\alpha$  in the experiment can be controlled by temperature and its typical values vary between 0.1 and 0.02.

There are two types of coupling between cells in a ladder. The first is the inductive coupling between the cells that is expressed by the self-inductance parameter  $\beta_L = 2\pi L I_{cV}/\Phi_0$ , where  $L$  is the self-inductance of the elementary cell. The second is the nonlinear Josephson coupling via horizontal junctions. The ratio of the horizontal and vertical junction areas is called the anisotropy factor and can be expressed in terms of the junction critical currents  $\eta = I_{cH}/I_{cV}$ . If this factor is equal to zero, the vertical junctions are decoupled and operate independently one from another. On the other hand, if this factor goes to infinity the ladder behaves like a parallel one-dimensional array and no rotobreather can exist since no magnetic flux can enter through the horizontal junctions. Thus, it is an important challenge to increase the anisotropy as far as possible. In this work we present measurements for the highest anisotropy factor ( $\eta = 0.56$ ) studied up to now. In contradiction to the existing theoretical prediction<sup>10</sup> for this anisotropy value, in the studied parameter range with moderate dissipation we find a rich diversity of localized excitations.

To briefly introduce the role of parameters we like to quote the equations of motion for our system (see Ref. 9 for details):

$$\ddot{\varphi}_l^V + \alpha \dot{\varphi}_l^V + \sin \varphi_l^V = \gamma - \frac{1}{\beta_L}(-\Delta \varphi_l^V + \nabla \tilde{\varphi}_{l-1}^H - \nabla \varphi_{l-1}^H), \quad (1)$$

$$\dot{\varphi}_l^H + \alpha \dot{\varphi}_l^H + \sin \varphi_l^H = -\frac{1}{\eta \beta_L}(\varphi_l^H - \tilde{\varphi}_l^H + \nabla \varphi_l^V), \quad (2)$$

$$\ddot{\tilde{\varphi}}_l^H + \alpha \dot{\tilde{\varphi}}_l^H + \sin \tilde{\varphi}_l^H = \frac{1}{\eta \beta_L}(\varphi_l^H - \tilde{\varphi}_l^H + \nabla \varphi_l^V), \quad (3)$$

where  $\varphi_l^V$ ,  $\varphi_l^H$ ,  $\tilde{\varphi}_l^H$  are the phase differences across the  $l$ th vertical junction and its right upper and lower horizontal neighbors,  $\nabla \varphi_l = \varphi_{l+1} - \varphi_l$ ,  $\Delta \varphi_l = \varphi_{l+1} + \varphi_{l-1} - 2\varphi_l$ , and  $\gamma = I_B/I_{cV}$  is the normalized bias current.

In order to generate a discrete breather in a ladder we used the technique described in Ref. 7. We used two extra bias leads for the middle vertical Josephson junction (cf. Fig. 1(b)) to apply a local current  $I_{local} > I_{cV}$ . This current switches the vertical junction in the resistive state. At the same time, being forced by magnetic flux conservation, one or two horizontal junctions on both sides of the vertical junctions also switch to the resistive state. After that  $I_{local}$  is reduced and, simultaneously, the uniform bias  $I_B$  is tuned up. In the final state, we keep the bias  $I_B$  smaller than  $I_{cV}$  and have reduced  $I_{local}$  to zero. By changing the starting value of  $I_{local}$  it is possible

to get more than one vertical junction rotating. When trying the slightly different current sweep sequence described in Ref. 6 we generated mainly states with many rotating vertical junctions.

In all measurements presented below, we have measured the dc voltage across the middle vertical junction as a function of the homogeneous bias current  $I_B$ . We used the method of low temperature scanning laser microscopy<sup>12</sup> to obtain electrical images from the dynamic states of the ladder. The laser beam locally heats the sample and changes the dissipation in an area of several micrometers in diameter. If the junction at the heated spot is in the resistive state, a voltage change will be measured. By scanning the laser beam over the whole ladder we can visualize the rotating junctions.

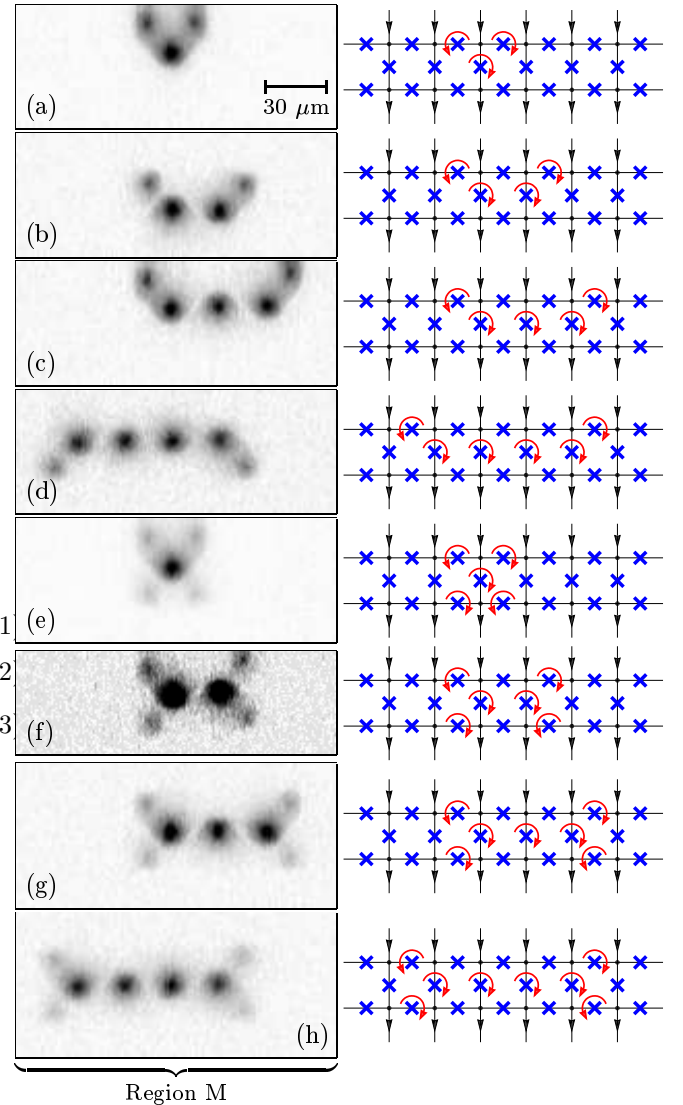


FIG. 2. Various localized states (discrete rotobreathers) measured by the low temperature scanning laser microscope: (a)–(d) asymmetric rotobreathers, (e)–(h) symmetric rotobreathers. Region M is illustrated in Fig. 1(b).

Various measured ladder states are shown in Fig. 2 as 2D gray scale maps. The gray scale corresponds to the measured voltage response during the laser scanning. In Fig. 2(a) we present the simplest of observed states, an *asymmetric* single-site rotobreather, where one vertical Josephson junction and the upper adjacent horizontal Josephson junctions are in the resistive state. On the right side of the plot we show the corresponding schematic view with arrows marking the rotating junctions. In the case of Fig. 2(b) two vertical junctions and two horizontal junctions are rotating that corresponds to an asymmetric two-site breather. An asymmetric three-site breather and an asymmetric four-site breather are shown in Fig. 2(c) and (d) respectively. Here, the voltage of the whirling horizontal and vertical junctions are equal due to magnetic flux conservation. The magnetic flux enters the ladder through one horizontal junction, goes through the vertical ones and leaves the ladder through another horizontal junction. When a single magnetic flux quantum is passing through a Josephson junction its phase  $\varphi$  is changing by  $2\pi$ . In contrast to our previous measurements of an annular ladder<sup>7</sup>, here in ladders with open boundaries we observe asymmetric breathers as frequently as symmetric breathers. The  $I_B$ - $V$  characteristics of these localized states is presented in Fig. 3(a). Particular states indicated on the plot are stable along the measured curves. The more junctions are whirling, the higher is the measured resistance.

Another type of discrete breathers observed in our experiment is shown in the Fig. 2(e)–(h). Figure 2(e) illustrates a *symmetric* single-site breather with one vertical and all four adjacent horizontal junctions are in the resistive state. Though we call this states symmetric, the upper and the lower horizontal junctions may in general have different voltages. The simplest voltage-symmetric case would be when each horizontal junction voltage is equal to half of the voltage of the whirling vertical junction<sup>7</sup>. We also observed a variety of multi-site breathers of this type. A two-site, a three-site, and a four-site breather is shown in Fig. 2 (f), (g), and (h), respectively. The corresponding  $I_B$ - $V$  characteristics over the stability range of symmetric breathers are presented in Fig. 3(b).

As mentioned above, Figs. 3(a) and (b) show the  $I_B$ - $V$  characteristics with  $I_{\text{local}} = 0$  of asymmetric and symmetric rotobreathers, respectively. The voltage  $V$  is always recorded locally on the middle vertical junction which was initially excited by the local current injection. The vertical line on the left side corresponds to the superconducting (static) state. The rightmost (also the bottom) curve accounts for the spatially uniform whirling state (all vertical junctions rotate synchronously and horizontal junctions are not rotating). An electrical image of this state is shown in Fig. 1(c). The upper branches in Fig. 3 represent various localized states. The uppermost branch corresponds to an single-site breather, the next lower branch to a two-site breather, and so on.

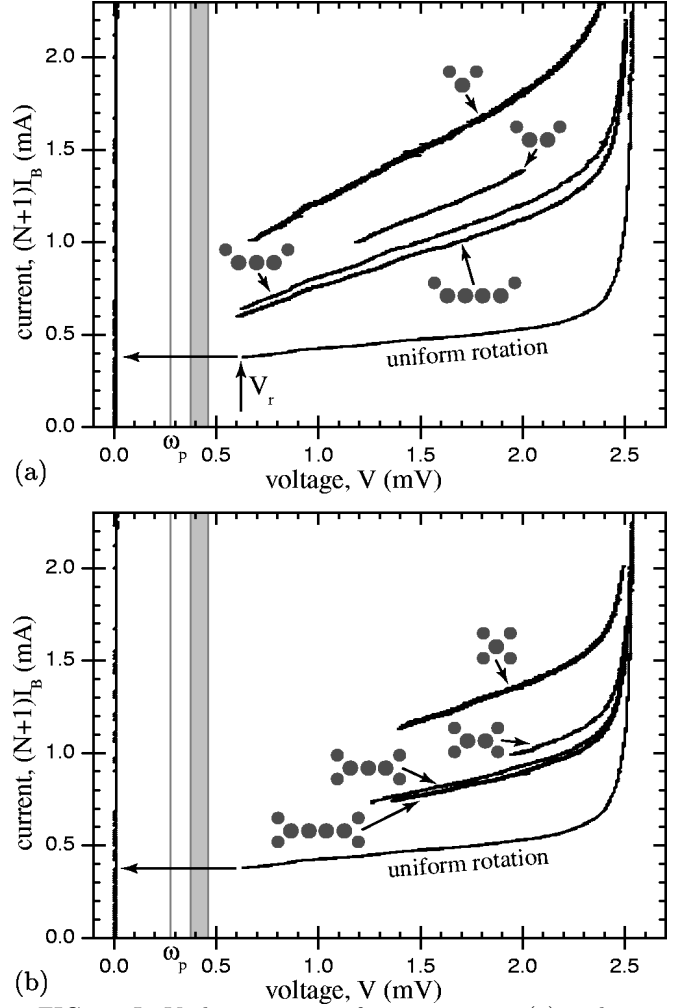


FIG. 3.  $I_B$ - $V$  characteristics for asymmetric (a) and symmetric (b) breathers in a ladder with the parameters  $N = 10$ ,  $I_{cV} = 320 \mu\text{A}$ ,  $\eta = 0.56$ , and  $\beta_L = 4.3$ . The grey region indicates the frequency range of the upper plasmon band.  $\omega_p$  is the plasma frequency.

It is easy to show that the voltage  $V_r$  at which the vertical and horizontal junctions switch back to the superconducting state is the same. By using  $R_{\text{sgV}}/R_{\text{sgH}} = \eta$  and  $I_{cH}/I_{cV} = \eta$  we get with  $I_r \propto I_c$  that  $V_r = R_{\text{sgV}}I_{rV} = R_{\text{sgH}}I_{rH}$ . For the uniform state we observed  $V_r \approx 0.6$  mV. At about the same voltage, the whirling horizontal and vertical junctions for the asymmetric breather are retrapped to the static state as can be seen in Fig. 3(a). The symmetric breathers show different behavior. Assuming  $V_H \approx V_V/2$ , we can expect that already at the voltage  $V = 2V_r \approx 1.2$  mV the horizontal junctions should trap into the superconducting state. But if the voltages of the top and bottom horizontal junctions are not equal while decreasing  $I_B$ , the retrapping current in the junction with the lower voltage is reached earlier and the retrapping occurs at a higher measured voltage.

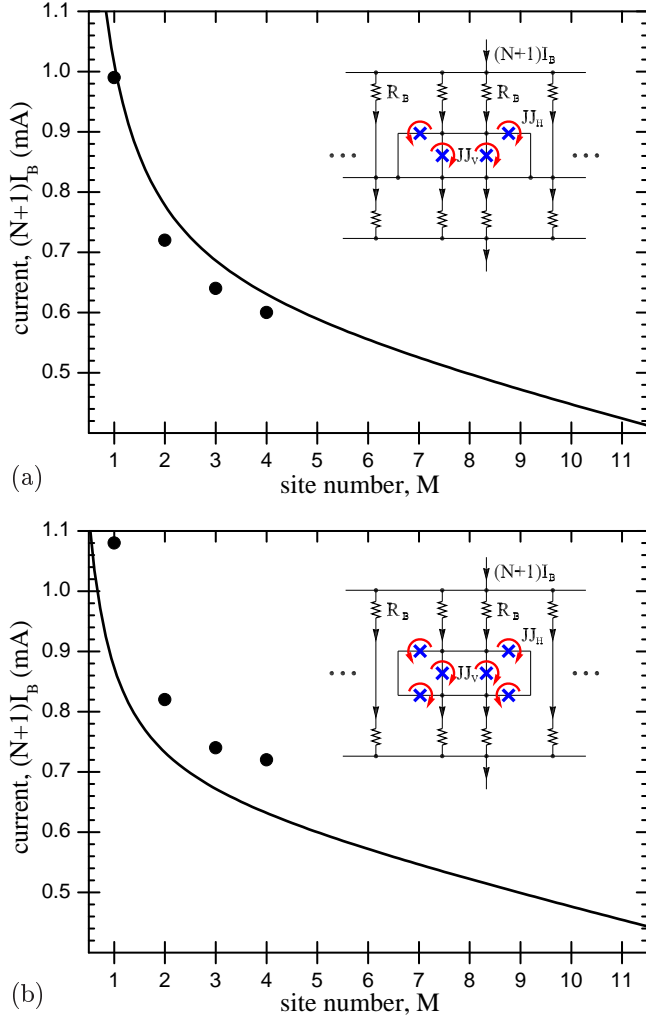


FIG. 4. The retrapping current measured (points) and calculated (line) by Eq. (4) for the asymmetric (a) ( $V = V_r$ ) and the symmetric (b) ( $V = 2V_r$ ) rotobreathers. The insets show the reduced electric circuits for each case.

We found that in order to explain the retrapping current of the breather states the bias resistors  $R_B$  have to be taken into account. Initially, these resistors have been designed for providing a uniform bias current distribution in the ladder. Assuming that the Josephson junctions in the superconducting state are just short circuits we get the electric circuits which are shown as insets in Fig. 4. The total current injected in the breather region is calculated by using the resistance  $R$  of vertical junctions measured in the spatially-uniform state. Thus we derive the retrapping current as

$$(N+1)I_B = \left[ \frac{(N-M+1)}{(1+\delta)R_B} + \frac{(N+1)[M+(2-\delta)\eta]}{MR} \right] V, \quad (4)$$

where  $M$  is the number of whirling vertical junctions. The parameter  $\delta$  is equal to 0 for asymmetric breathers and to 1 for symmetric breathers. The calculated retrap-

ping current is compared with the experiment in Fig. 4. For the asymmetric breathers the agreement is fairly good. We believe that the larger discrepancy for the symmetric breathers is due to the assumption  $V_H = V_V/2$  that we imposed in derivation of the retrapping current.

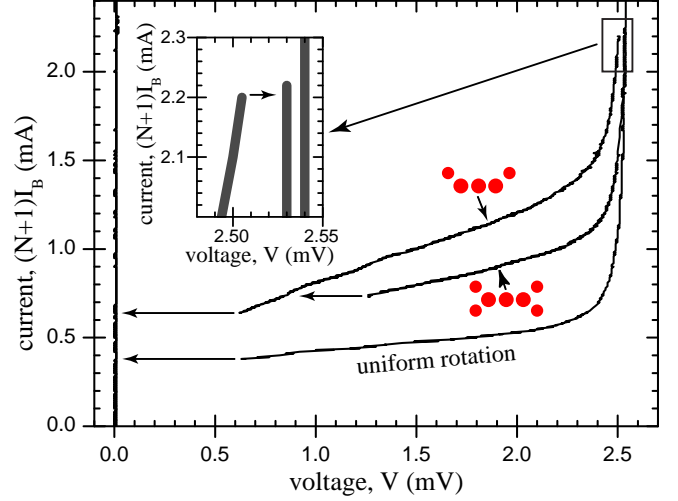


FIG. 5.  $I_B$ - $V$  characteristics of three-site breathers.

One interesting feature in our experiment is the dynamical behavior of the local states in the linear ladder which differs from the previous observations in the annular ladder<sup>7</sup> with the anisotropy parameter  $\eta = 0.44$ . In Fig. 5 this feature is illustrated for 3-site breathers. After the creation of a symmetric rotobreather (middle curve) we are lowering the uniform bias current  $I_B$  until the retrapping current of one of the horizontal junctions at each side is reached. Here we observe switching to the corresponding asymmetric 3-site rotobreather state. By further lowering of the bias current we get to the point where both the vertical and the horizontal junctions reach their retrapping currents and the whole ladder goes into the superconducting state. If, instead of lowering the bias current, we start increasing it another switching point is observed where the previous symmetric breather state is recovered. In contrast to this behavior, in the annular ladder<sup>7</sup> the observed lower instability of the symmetric breather led to an *increase* of voltage. Moreover, this switching turned the number of rotating junctions to increase, with few more vertical junctions starting to rotate.

In addition to the simplest hierarchic states described above we also found a large variety of more complex localized dynamic states. Some examples are presented in Fig. 6. Fig. 6(a)-(c) are sections from the middle region ( $M$ ) [cf. Fig. 1(b)] of the measured linear ladder. Fig. 6(a) shows an asymmetric 6-site breather with top and bottom horizontal junctions whirling on its sides. Fig. 6(b) illustrates a 3-site rotobreather which is symmetric on one side and asymmetric on the other. Another very peculiar localized state is presented in Fig. 6(c).

The rightmost vertical junction is rotating with a lower frequency than the other four vertical junctions on the left. This can be understood from the appearance of an extra rotating horizontal junction in the interior of this state. We can interpret it as a 4-site breather coupled to a single-site breather. All these localized states would be topologically forbidden in the case of an annular ladder as the magnetic flux inside the superconducting circuit should not accumulate, but they are not forbidden in a ladder with open boundaries. The last two pictures (d) and (e) are taken near the border of the ladder. We find here truncated asymmetric and symmetric 6-site breathers. The marginal vertical junction does not require any horizontal junctions to rotate.

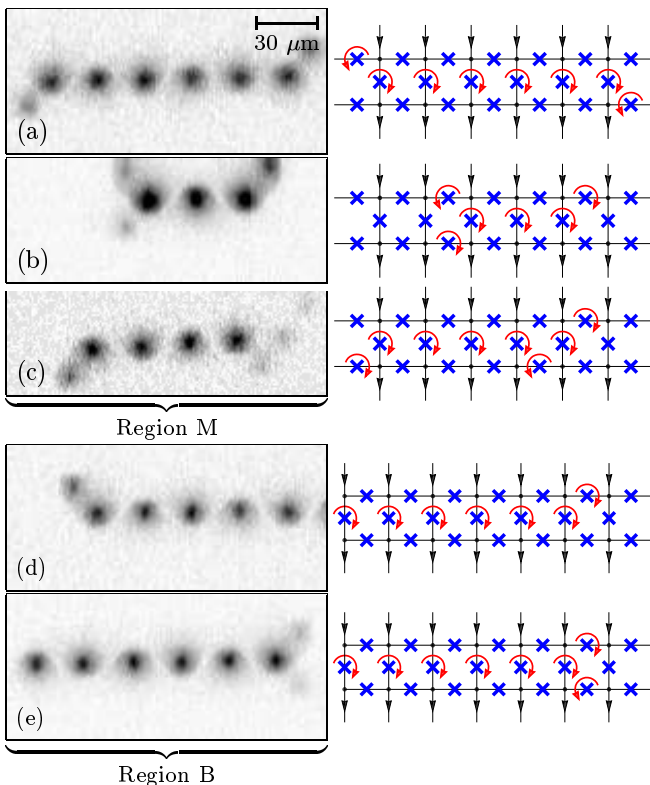


FIG. 6. More complex non-uniform states measured in the middle (M) and on the border (B) regions of the ladder.

In summary, we presented observation of a large variety of spatially-localized dynamic rotobreather states in Josephson ladders with open boundaries. These states can be excited by the local current injection and supported by the uniform current bias. We observe both symmetric and asymmetric rotobreather states predicted in Ref. 10, as well as more complex mixed states. We believe that the region of existence and stability of rotobreathers does sensitively depend on dissipation, discreteness, and anisotropy parameter of the ladder.

- <sup>1</sup> S. Aubry, *Physica D* **103**, 201 (1997).
- <sup>2</sup> S. Flach and C. R. Willis, *Phys. Rep.* **295**, 181 (1998).
- <sup>3</sup> B. I. Swanson, J. A. Brozik, S. P. Love, G. F. Strouse, A. P. Shreve, A. R. Bishop, W.-Z. Wang, and M. I. Salkola, *Phys. Rev. Lett.* **82**, 3288 (1999).
- <sup>4</sup> U. T. Schwarz, L. Q. English, and A. J. Sievers, *Phys. Rev. Lett.* **83**, 223 (1999).
- <sup>5</sup> H. S. Eisenberg, Y. Silberberg, R. Morandotti, A. R. Boyd, and J. S. Aitchison, *Phys. Rev. Lett.* **81**, 3383 (1998).
- <sup>6</sup> E. Trías, J. J. Mazo, and T. P. Orlando, *Phys. Rev. Lett.* **84**, 741 (2000).
- <sup>7</sup> P. Binder, D. Abraimov, A. V. Ustinov, S. Flach, and Y. Zolotaryuk, *Phys. Rev. Lett.* **84**, 745 (2000).
- <sup>8</sup> L. M. Floría, J. L. Marin, P. J. Martinez, F. Falo, and S. Aubry, *Europhys. Lett.* **36**, 539 (1996).
- <sup>9</sup> S. Flach and M. Spicci, *J. Phys.: Condens. Matter* **11**, 321 (1999).
- <sup>10</sup> J. J. Mazo, E. Trías, and T. P. Orlando, *Phys. Rev. B* **59**, 13604 (1999).
- <sup>11</sup> HYPRES Inc., Elmsford, NY 10523.
- <sup>12</sup> A. G. Sivakov, A. P. Zhuravel', O. G. Turutanov, I. M. Dmitrenko, *Appl. Surf. Sci.* **106**, 390 (1996).